Electron transport through double quantum dots with spin-polarization dependent interdot coupling

2008 J. Phys.: Condens. Matter 20 085214

(http://iopscience.iop.org/0953-8984/20/8/085214)

IOP PUBLISHING JOURNAL OF PHYSICS: CONDENSED MATTER

J. Phys.: Condens. Matter **20** (2008) 085214 (6pp) doi:10.1088/0953-8984/20/8/085214

Electron transport through double quantum dots with spin-polarization dependent interdot coupling

Zhi-Jian Li, Yan-Hong Jin, Yi-Hang Nie and Jiu-Qing Liang

Institute of Theoretical Physics and Department of Physics, Shanxi University, Taiyuan 030006, People's Republic of China

Received 23 May 2007, in final form 10 January 2008
Published 1 February 2008
Online at stacks.iop.org/JPhysCM/20/085214

Abstract

By means of Green functions within the equation of motion scheme, we theoretically investigate electron transport through two lateral quantum dots between which spin-dependent tunneling occurs. In the presence of intradot Coulomb interactions, the expressions for spin and charge currents are given under the Hartree–Fock approximation. The magnitude and polarization of the spin current can be controlled critically by adjusting the gate voltage applied over the quantum dots. The variation of the spin current and the charge current versus the gate voltage can be qualitatively explained by a spin-dependent resonant tunneling picture.

1. Introduction

In recent years the study of spintronic devices, which utilize the spin rather than the charge of an electron, has been intensified. They are expected to operate at much higher speeds than conventional devices and have potential applications in quantum computing [1, 2]. Finding novel ways to generate, control and utilize the spin-polarized current is of great importance in designing and manufacturing spintronic devices. Spin polarization occurs naturally in any material with an imbalance of the spin populations at the Fermi level, so ferromagnetic metals usually act as a source of spin injection to a semiconductor [3–6]. Also a spin current arises in the electron system with substantial spin–orbit interaction. One kind of spin–orbit interaction originates from the coupling of conduction electrons and localized spins of impurities. When an unpolarized electron beam is scattered by an impurity it becomes polarized perpendicular to the plane of scattering. Further scattering of this polarized beam is asymmetric for electrons with opposite spin polarizations. Thus a transverse spin current arises [7, 8]. The other kind of spin–orbit interaction is intrinsic in conventional hole-doped semiconductors or in two-dimensional semiconductor heterostructures. The spin Hall effect and other transport characteristics have been widely studied in these systems [9–11].

In this paper we focus on the quantum-dot structure which is another system for studying spin-polarization transport. Devices consisting of quantum dots have undergone considerable investigation from a theoretical viewpoint [12–16]. In most of these studies, a spin-polarized current is induced by either a rotating magnetic field applied directly to the quantum dot or a ferromagnetic lead. Here we suggest a new device, a lateral double quantum dot with spin-dependent interdot coupling, that produces spin-polarized current. Technically spin-dependent interdot coupling can be achieved by applying a constant magnetic field on the tunneling junction between two quantum dots [17]. This magnetic field make the electron spin perform Larmor precession when it passes through the potential barrier. An electron with spin parallel to the magnetic field has a larger tunneling probability than one with spin antiparallel to the magnetic field [18]. As a result, a spin-polarized current is produced. Using the Keldysh nonequilibrium Green function technique and employing the Hartree–Fock approximation, we derive expressions for spin-resolved currents. For a strongly coupled double quantum dot we demonstrate numerically that the magnitude and polarization of the spin current is tunable via a gate voltage. The variation of spin current versus the gate voltage can be qualitatively explained by a spin-dependent resonant tunneling model.

2. Model and formula

The considered system of the double quantum dots coupled in series to two normal metal leads is presented in figure 1. The intradot Coulomb interaction is scaled by energy U while the

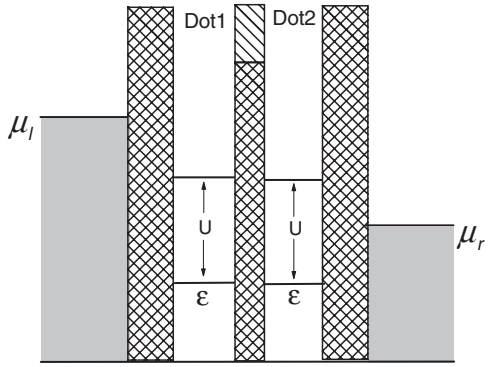

Figure 1. Energy sketch of the lateral double quantum dot coupled to two mental leads. The potential barrier between two quantum dots is spin-dependent.

interdot Coulomb interaction is neglected. The tunnel coupling between two quantum dots is spin-dependent. The second quantized Hamiltonian corresponding to our model is written as

$$H = H_{\rm d} + H_\alpha + H_{\rm T}, \tag{1}$$

with

$$H_{\rm d} = \sum_{m\sigma} \varepsilon_{m\sigma} d^\dagger_{m\sigma} d_{m\sigma} + \sum_m U n_{m\uparrow} n_{m\downarrow} + \sum_\sigma [(t + \sigma\Delta t) d^\dagger_{1\sigma} d_{2\sigma} + \text{H.c.}] \qquad (m = 1, 2), \tag{2}$$

$$H_\alpha = \sum_{\alpha k\sigma} \varepsilon_{\alpha k\sigma} c^\dagger_{\alpha k\sigma} c_{\alpha k\sigma} \qquad (\alpha = l, r), \tag{3}$$

$$H_{\rm T} = \sum_{k\sigma} (V_{lk1} c^\dagger_{lk\sigma} d_{1\sigma} + V_{rk2} c^\dagger_{rk\sigma} d_{2\sigma} + \text{H.c.}). \tag{4}$$

Clearly $H_{\rm d}$ is due to the double quantum dot part, H_α describes the conduction electrons in the left and right leads, and $H_{\rm T}$ introduces the tunneling between dot and lead with the coupling matrix element $V_{\alpha km}$. Here $d^\dagger_{m\sigma}$ ($d_{m\sigma}$) is the creation (annihilation) operator for an electron with spin σ in the quantum dot m whereas $c^\dagger_{\alpha k\sigma}$ ($c_{\alpha k\sigma}$) are the corresponding operators in the left and right leads. $n_{m\sigma} = d^\dagger_{m\sigma} d_{m\sigma}$ is the particle number operator. The third term on the right-hand side of equation (2) gives the tunneling between the two quantum dots without spin flip. The tunneling coefficients $t = \int \varphi_1^*(x)(\frac{p^2}{2m} + V)\varphi_2(x)\,{\rm d}x$ and $\Delta t = \frac{1}{2} g\mu_{\rm B} B \int \varphi_1^*(x)\varphi_2(x)\,{\rm d}x$, where $\varphi_m(x)$ is the space wavefunction of each quantum dot. As mentioned in the introduction, it is considered that Δt is induced by a static magnetic field applied to the barrier region between two quantum dots. In our considerations we assume the excitation energy to be very large and only two energy levels $\varepsilon_{m\sigma}$ and $\varepsilon_{m\sigma} + U$ to be in each quantum dot.

In our model there are no origins inducing spin-flip, so the spin-resolved current I_σ through the system is uniform in the steady state regime. That is to say, the spin-resolved current $I_{{\rm r}\sigma}$ from the right lead is opposite to the current $I_{{\rm l}\sigma}$ from the left lead, i.e. $I_\sigma = I_{{\rm r}\sigma} = -I_{{\rm l}\sigma}$ [19]. This current can be calculated in terms of the Green functions of coupling quantum dots (see the appendix)

$$I_\sigma = -e\,{\rm Im}\left[\int \frac{{\rm d}\omega}{2\pi} \Gamma_{r2}(\omega)[2G^r_{2\sigma,2\sigma}(\omega) f_r(\omega) + G^<_{2\sigma,2\sigma}(\omega)]\right], \tag{5}$$

where $f_\alpha(\varepsilon_{\alpha k\sigma}) = [\exp[(\varepsilon_{\alpha k\sigma} - \mu_\alpha)/(k_{\rm B}T)] + 1]^{-1}$ is the Fermi distribution function of electrons in the lead α with chemical potential μ_α, temperature T and Boltzmann constant $k_{\rm B}$. $\Gamma_{\alpha m}(\omega) = 2\pi \sum_k |V_{\alpha km}|^2 \delta(\omega - \varepsilon_{\alpha k})$ is the linewidth function and we have assumed that the energy $\varepsilon_{\alpha k\sigma}$ of the conduction electrons in leads is spin-degenerate, i.e. $\varepsilon_{\alpha k} = \varepsilon_{\alpha k\sigma}$. $G^r_{22\sigma\sigma}(\omega)$ and $G^<_{22\sigma\sigma}(\omega)$ are the Fourier transform of standard retarded Green function $G^r_{m\sigma,n\sigma'}(t, t') \equiv \langle\langle d_{m\sigma}(t)|d^\dagger_{n\sigma'}(t')\rangle\rangle^r \equiv -{\rm i}\theta(t - t')\langle\{d_{m\sigma}(t), d^\dagger_{n\sigma'}(t')\}\rangle$ and lesser Green function $G^<_{m\sigma,n\sigma'}(t, t') = \langle\langle d_{m\sigma}(t)|d^\dagger_{n\sigma'}(t')\rangle\rangle^< \equiv {\rm i}\langle d^\dagger_{n\sigma'}(t') d_{m\sigma}(t)\rangle$, respectively. In the basis $|1\uparrow\rangle$, $|2\uparrow\rangle$, $|1\downarrow\rangle$ and $|2\downarrow\rangle$, they can be calculated through the Dyson equation and Keldysh equation, i.e.

$$G^r(\omega) = g^r(\omega) + g^r(\omega)\Sigma^r G^r(\omega), \tag{6}$$

$$G^<(\omega) = G^r(\omega)\Sigma^< G^a(\omega), \tag{7}$$

respectively, where

$$G^r(\omega) = \begin{pmatrix} G^r_{1\uparrow1\uparrow} & G^r_{1\uparrow2\uparrow} & G^r_{1\uparrow1\downarrow} & G^r_{1\uparrow2\downarrow} \\ G^r_{2\uparrow1\uparrow} & G^r_{2\uparrow2\uparrow} & G^r_{2\uparrow1\downarrow} & G^r_{2\uparrow2\downarrow} \\ G^r_{1\downarrow1\uparrow} & G^r_{1\downarrow2\uparrow} & G^r_{1\downarrow1\downarrow} & G^r_{1\downarrow2\downarrow} \\ G^r_{2\downarrow1\uparrow} & G^r_{2\downarrow2\uparrow} & G^r_{2\downarrow1\downarrow} & G^r_{2\downarrow2\downarrow} \end{pmatrix}, \tag{8}$$

$$g^r(\omega) = \begin{pmatrix} g_{1\uparrow} & 0 & 0 & 0 \\ 0 & g_{2\uparrow} & 0 & 0 \\ 0 & 0 & g_{1\downarrow} & 0 \\ 0 & 0 & 0 & g_{2\downarrow} \end{pmatrix}, \tag{9}$$

and $G^a(\omega)$ is the corresponding advanced Green function. $g^r(\omega)$ denotes the retarded Green function of uncoupled dots with the matrix elements

$$g_{m\sigma} = \frac{\omega - \varepsilon_{m\sigma} - U + U\langle n_{m\bar\sigma}\rangle}{(\omega - \varepsilon_{m\sigma})(\omega - \varepsilon_{m\sigma} - U)}, \tag{10}$$

in which the average values of the occupation numbers $\langle n_{m\sigma}\rangle = \langle d^\dagger_{m\sigma}(t) d_{m\sigma}(t)\rangle$ need to be calculated self-consistently by using the formula

$$\langle n_{m\sigma}\rangle = -{\rm i}\int \frac{{\rm d}\omega}{2\pi} G^<_{m\sigma m\sigma}(\omega). \tag{11}$$

The self-energy $\Sigma^r(\omega)$ in equation (6) can be obtained by the standard equation of motion technique (see the appendix). Under the Hartree–Fock approximation, it has the form

$$\Sigma^r(\omega) = \begin{pmatrix} \Sigma_{1\uparrow} & (t + \Delta t) & 0 & 0 \\ (t + \Delta t) & \Sigma_{2\uparrow} & 0 & 0 \\ 0 & 0 & \Sigma_{1\downarrow} & (t - \Delta t) \\ 0 & 0 & (t - \Delta t) & \Sigma_{2\downarrow} \end{pmatrix} \tag{12}$$

with $\Sigma_{m\sigma} = \frac{-{\rm i}}{2}\Gamma_{\alpha m}\delta_{m1}\delta_{\alpha l} + \frac{-{\rm i}}{2}\Gamma_{\alpha m}\delta_{m2}\delta_{\alpha r}$. And the lesser self-energy is given by

$$\Sigma^< = -(\Sigma^r - \Sigma^a)(\delta_{m1}\delta_{\alpha l} + \delta_{m2}\delta_{\alpha r}) f_\alpha = \begin{pmatrix} {\rm i}\Gamma_{l1} f_l & 0 & 0 & 0 \\ 0 & {\rm i}\Gamma_{r2} f_r & 0 & 0 \\ 0 & 0 & {\rm i}\Gamma_{l1} f_l & 0 \\ 0 & 0 & 0 & {\rm i}\Gamma_{r2} f_r \end{pmatrix}. \tag{13}$$

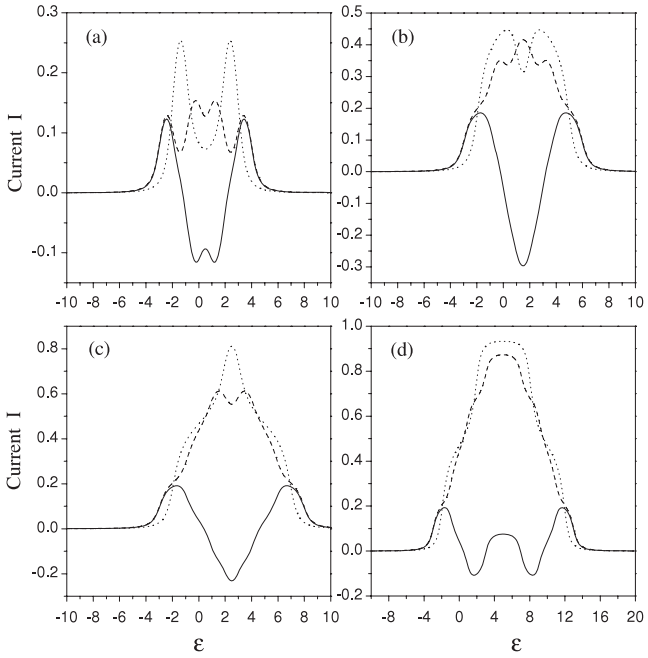

Figure 2. The electric current (dashed line) and the spin current (solid line) versus the gate voltage ε for noninteracting electrons with $t = 2$, $\Delta t = 1$ and (a) $V = 1$, (b) $V = 3$, (c) $V = 5$, (d) $V = 10$. The dotted line as a reference curve of electric current for the case $\Delta t = 0$.

In our consideration, the interesting currents are the charge current I_e and the spin current I_s, which are defined by

$$I_e = I_\uparrow + I_\downarrow \tag{14}$$

and

$$I_s = I_\uparrow - I_\downarrow, \tag{15}$$

respectively.

3. Numerical result and discussion

Once the retarded and lesser Green functions for an electron at the double quantum dot are known, the current and its transport properties can be determined using equation (5). In the following we present the numerical results for the currents concerned. In the wide-band limit, Γ_{l1} and Γ_{r2} are independent of energy ω and we assume $\Gamma_{l1} = \Gamma_{r2} = 1$ as an energy unit. The bare energy levels $\varepsilon_{m\sigma}$ of quantum dots are spin-degenerate and the energy levels belonging to different dots are set to be equal by adjusting the gate voltage, i.e. $\varepsilon_{m\sigma} = \varepsilon$. The bias voltage V is applied to the left electrode, so that $\mu_l = V$ while μ_r is kept constant equal to zero. The temperature is assumed to be $k_B T = 0.01$.

We first consider the case of noninteracting electrons, i.e. $U = 0$ in Hamiltonian H_d. With $t = 2$ and $\Delta t = 1$, figure 2 shows the electric current I_e (dash line) and spin current I_s (solid line) as a function of the position of the dot energy ε for selected values of the bias voltage V. The dotted line gives a reference curve for electric current for the case $\Delta t = 0$. The sign of the spin current indicates its polarization. The resonances of spin current with opposite polarization are displayed, which may serve as a guideline to construct a novel class of spintronic devices. To explain the origin of the resonances we employ a spin-dependent resonant tunneling picture. In the basis $\{|1\uparrow\rangle, |2\uparrow\rangle, |1\downarrow\rangle, |2\downarrow\rangle\}$, the Hamiltonian H_d has the matrix form

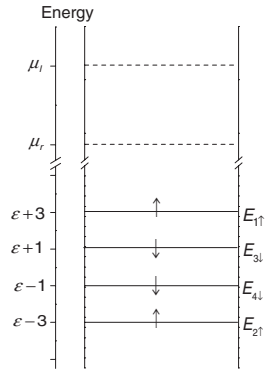

Figure 3. The schematic eigenenergies of the equivalent single quantum dot for the case of noninteracting electrons and a bias window between μ_r and μ_l. The parameters are the same as in figure 2.

$$H_d = \begin{bmatrix} \varepsilon & t+\Delta t & 0 & 0 \\ t+\Delta t & \varepsilon & 0 & 0 \\ 0 & 0 & \varepsilon & t-\Delta t \\ 0 & 0 & t-\Delta t & \varepsilon \end{bmatrix} \tag{16}$$

with four eigenvalues $E_{1\uparrow} = \varepsilon + t + \Delta t$, $E_{3\downarrow} = \varepsilon + t - \Delta t$, $E_{4\downarrow} = \varepsilon - t + \Delta t$ and $E_{2\uparrow} = \varepsilon - t - \Delta t$. For chosen parameters $t = 2$ and $\Delta t = 1$, the distance between two near eigenenergy levels is 2 and $E_{1\uparrow} > E_{3\downarrow} > E_{4\downarrow} > E_{2\uparrow}$. As shown in figure 3, the coupling double quantum dot for noninteracting electrons can be equivalent to one single quantum dot with four energy levels, two levels occupied by spin-up electrons and two levels by spin-down electrons. In fact, the isolated energy levels expand to energy bands due to the coupling of quantum dots and leads. The width of the energy band is determined by the coupling strength. The transport channels are supplied by the energy bands lying in the bias window, hence the currents in figures 2(a)–(d) appear at the same position of dot energy but disappear at different positions because of the bias voltage windows with fixed underside $\mu_r = 0$ and selected upper side $\mu_l = V$. As an illustrative example we explain the variations of current in figure 2(a) where the width of the bias window is 1. In the beginning, four equivalent energy bands are all below the window, so the electric current and the spin current are zero. With increasing gate voltage ε, the band edge of $E_{1\uparrow}$ first enters the bias window and a positive spin current appears. When $\varepsilon = -2.5$, the center of band $E_{1\uparrow}$ is in the middle of the bias window, so the positive spin current reaches a maximum. By further increasing ε, the energy band $E_{1\uparrow}$ exits the bias window while the energy band $E_{3\downarrow}$ enters it. Accordingly, the positive spin current decreases and the negative spin current increases. The positive spin current does not revive until the energy band $E_{2\uparrow}$ enters the bias window. When four eigenenergy bands pass through the bias window, the currents become zero.

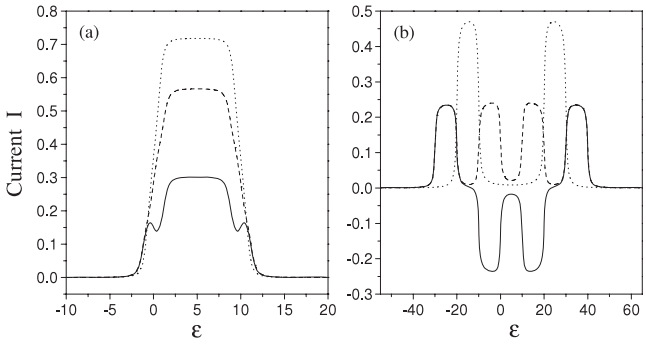

Figure 4. The electric current (dashed line) and the spin current (solid line) versus the gate voltage ε for noninteracting electrons with (a) $t = 0.8$, $\Delta t = 0.5$ and (b) $t = 20$, $\Delta t = 10$. Other parameters are the same as in figure 2(d). The dotted line is a reference curve for electric current for the case $\Delta t = 0$.

In figures 2(b) and (c), the width of the bias window is 3 and 5, respectively. Two energy bands, $E_{3\downarrow}$ and $E_{4\downarrow}$, occupied by spin-down electrons, can reside in the bias window together, so there is only one larger resonant valley for negative spin current. As the width of bias window is increased to 10 (figure 2(d)), four energy bands can be contained in it together. However, the spin current is not zero but positive for this configuration. The reason is that the spin-up transport channels are more effective than the spin-down transport channels due to the spin-dependent coupling $t \pm \Delta t$ between two quantum dots. This also explains why the absolute values of maximal positive spin current is larger than that of minimal negative spin current in figures 2(a) and (d), for example $\mathrm{Max}(I_\mathrm{s}) = 0.123$ while $\mathrm{Min}(I_\mathrm{s}) = -0.116$ in figure 2(a).

Figure 4 displays the currents versus the position of the dot energy ε for other choices of parameters t and Δt with fixed chemical potential $\mu_\mathrm{l} = 10$ and $\mu_\mathrm{r} = 0$. If we take $t = 0.8$ and $\Delta t = 0.5$, the negative spin current cannot be obtained as shown in figure 4(a). When we choose $t = 20$ and $\Delta t = 10$, the completely polarized current, i.e. $I_\mathrm{e} = |I_\mathrm{s}|$, is observed interestingly in figure 4(b), which can guide the design of the spin switch device. In this situation, the coupling between two quantum dots is larger than that between the quantum dot and the lead so that the transport of electrons is dominated by the tunneling through the barrier between the quantum dot and lead. Therefore, the spin-up transport channels and the spin-down channels are almost equally effective.

Next, we study the case of interacting electrons. The average values $\langle n_{m\bar{\sigma}} \rangle$ in equation (10) must be calculated self-consistently via equation (11). In figure 5, we show the electric current and the spin current as a function of gate voltage ε for different Coulomb interaction U. The bias voltage is chosen as $V = 10$ and other parameters are the same as in figure 2. The variations of the currents can be explained qualitatively by an effective spin-dependent resonant tunneling picture analogous to the noninteracting case. Under the Hartree–Fock approximations, the coupled double quantum dot with intradot Coulomb interaction can be equivalent to a single quantum dot with eight energy levels, four occupied by spin-up electrons and four by spin-down electrons. These eight

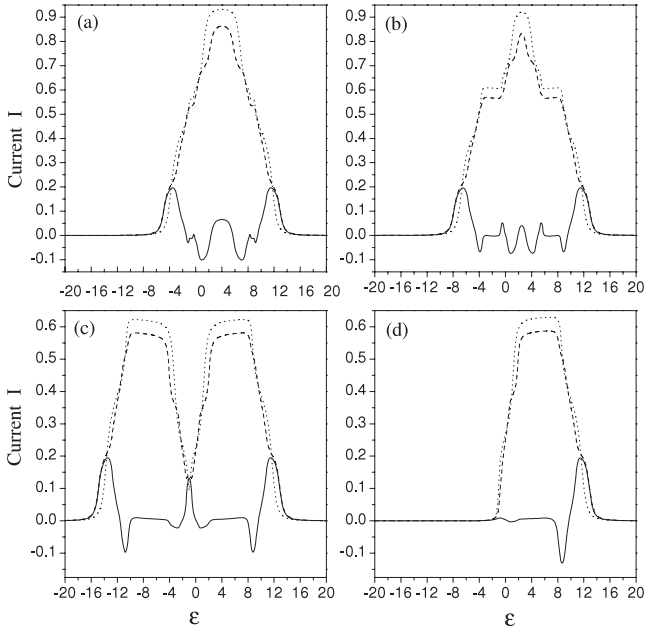

Figure 5. The electric current (dashed line) and the spin current (solid line) versus the gate voltage ε for interacting electrons with different Coulomb interaction: (a) $U = 2$, (b) $U = 5$, (c) $U = 12$ and (d) $U = \infty$. Other parameters are the same as in figure 2(d). The dotted line is a reference curve of electric current for the case $\Delta t = 0$.

energy levels are the poles of Green function $G^r(\omega)$, which can be obtained by solving the equation

$$|G^r(\omega)^{-1}| = |g^r(\omega)^{-1} - \tilde{\Sigma}^r(\omega)| = 0 \tag{17}$$

where

$$\tilde{\Sigma}^r(\omega) = \begin{pmatrix} 0 & (t+\Delta t) & 0 & 0 \\ (t+\Delta t) & 0 & 0 & 0 \\ 0 & 0 & 0 & (t-\Delta t) \\ 0 & 0 & (t-\Delta t) & 0 \end{pmatrix}, \tag{18}$$

and it comes from $\Sigma^r(\omega)$ without taking account of the coupling between the lead and the quantum dot. To solve equation (17), we first diagonalize $G^r(\omega)^{-1}$, then make the diagonal element equal to zero, so we can obtain four equations. Each equation has more than one solution due to $g^{-1}_{m\sigma}$ not being a linear function of ω. As a result, we can obtain eight different solutions for equation (17) in all, though $G^r(\omega)$ is a 4×4 matrix. Four of these solutions, which are functions of $t + \Delta t$, can be identified as the energy levels occupied by spin-up electrons. The other four solutions are functions of $t - \Delta t$ and the corresponding energy levels are occupied by spin-down electrons. It should be mentioned that there are also eight equivalent energy levels for the case of two electron states per quantum dot but without Coulomb interaction. These energy levels similar to figure 3 are independent of the occupation numbers $\langle n_{m\sigma} \rangle$, and their variations with ε have a parallel configuration. However, the eight eigenenergy levels we obtain depend on the occupation numbers $\langle n_{m\sigma} \rangle$ and they must be calculated numerically via equation (11). We take the example of $U = 5$ to illuminate the

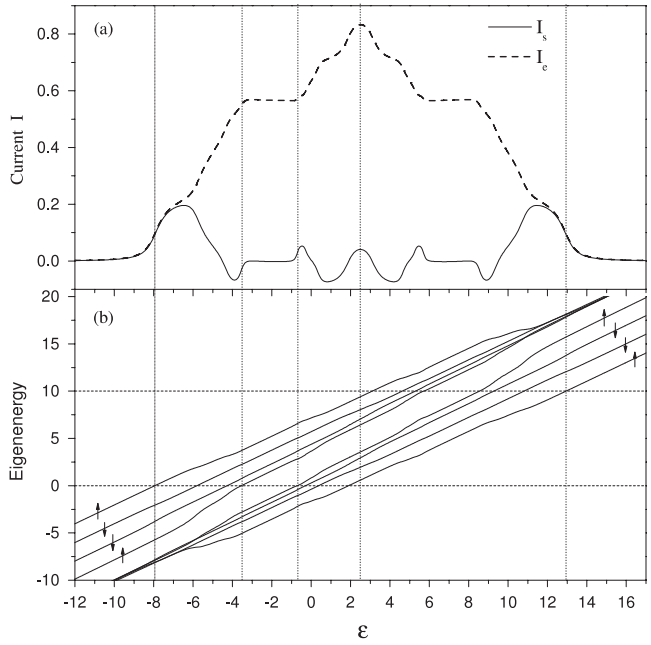

Figure 6. Part (a) is just figure 5(b). Part (b) depicts the eigenenergy of the equivalent single quantum dot for the case of interacting electrons as a function of the gate voltage ε. The space between two horizontal dashed lines is the bias voltage window.

variations of currents as shown in the figure 6(a). Figure 6(b) plots the eight equivalent eigenenergy levels as a function of gate voltage ε. The energy level occupied by spin-up (spin-down) electrons is indicated by an up-arrow $\uparrow$ (down-arrow $\downarrow$). With increasing gate voltage ε, the energy level occupied by spin-up electrons first enters the bias window about at $\varepsilon = -8$, meanwhile the electric current and the positive spin current have appeared due to the expansion of energy levels. When the gate voltage ε varies from -3.6 to -1.8, two spin-up energy levels and two spin-down energy levels are always in the bias window, so the electric current and spin current keep a plateau. At the symmetrical point of current, i.e. $\varepsilon = 2.5$, all eight energy levels become transport channels and the electric current reaches a maximum. Once ε departs from the symmetry point, a spin-up energy level first goes out from the bias window and as a result the spin current drops. By further increasing ε and up to the last energy level exiting the bias window, the electric current and spin current revert to zero asymptotically as expected.

It may be useful to estimate the practical value of the effective magnetic field for generation of spin-dependent coupling between two quantum dots in our system. For the temperature $k_BT = 0.01\Gamma$ and the linewidth function $\Gamma = 5\ \mu$eV in typical GaAs/AlGaAs quantum-dot experiments [20], the magnitude of the magnetic field corresponding to $\Delta t = \Gamma$ is $B \sim 0.17/g$ T, where g is effective electron g-factor. In our considerations we assume that a uniform magnetic field is just confined to the barrier region, which is experimentally difficult to do. In fact, if a spatially nonuniform magnetic field is applied to both the barrier region and the two quantum dots, a similar effect can be obtained when the magnetic field applied to the barrier region is strong but the magnetic field applied to quantum dots is weak compared to the linewidth function Γ. For this magnetic field configuration, the influence on quantum dots can be neglected and it should be experimentally feasible by using present technologies.

4. Conclusion

In summary, we have proposed a new structure, a lateral double quantum dot with spin-dependent interdot coupling in a gated semiconductor device, to generate a spin-polarized current. Unlike the usual quantum-dot spin device, where a rotating magnetic field is required to cause the spin flip, we suggest that the tunneling junction region between two quantum dots has a static magnetic field imposed or is made of ferromagnetic material. Using the Keldysh nonequilibrium Green function technique and employing the Hartree–Fock approximations, the expressions for spin-resolved currents are derived when considering the intradot Coulomb interaction. It is demonstrated numerically that the magnitude and the polarization of the spin-polarized current are tunable by adjusting the gate voltage applied over the quantum dots. Interesting resonance behavior of the spin-polarized currents is observed and can be qualitatively explained by a spin-dependent resonant tunneling model.

Acknowledgments

We gratefully acknowledge financial support from the Youth Sciences Foundation of Shanxi Province (2007021001), the Science and Technology Key Item of Chinese Ministry of Education (207017) and the National Natural Science Foundation of China (10774094).

Appendix. Deduction of the spin-resolved currents

The spin-resolved current in right lead is defined as

$$I_\sigma = -e\frac{\mathrm{d}}{\mathrm{d}t}\left\langle \sum_k c^\dagger_{rk\sigma}(t)c_{rk\sigma}(t)\right\rangle = 2ie\,\mathrm{Re}\left[\sum_k V_{rk2}\left\langle c^\dagger_{rk\sigma}(t)d_{2\sigma}(t)\right\rangle\right]. \tag{19}$$

According to the Langreth theorem [21], the quantum statistical average value $\langle c^\dagger_{rk\sigma}(t)d_{2\sigma}(t)\rangle$ can be expressed as

$$\left\langle c^\dagger_{\alpha k\sigma}(t)d_{m\sigma}(t')\right\rangle = -\mathrm{i}\int \mathrm{d}t_1 V^*_{\alpha km}[G^r_{m\sigma,m\sigma}(t,t_1)g^<_{\alpha k\sigma}(t_1,t') + G^<_{m\sigma,m\sigma}(t,t_1)g^a_{\alpha k\sigma}(t_1,t')], \tag{20}$$

where $g^a_{\alpha k\sigma}(t_1,t') = \mathrm{i}\theta(t'-t)\exp[-\mathrm{i}\varepsilon_{\alpha k\sigma}(t-t')]$ and $g^<_{\alpha k\sigma}(t_1,t') = \mathrm{i}f_\alpha(\varepsilon_{\alpha k\sigma})\exp[-\mathrm{i}\varepsilon_{\alpha k\sigma}(t-t')]$ are advanced and lesser Green functions for free electrons in the leads, respectively. Making a Fourier transform to equation (20), the spin-resolved current formula equation (5) is obtained.

To determine the currents through the double-dot system, we solve the retarded Green function $G^r_{m\sigma,n\sigma'}(\omega)$ in equation (5) by a standard equation of motion technique

$$\omega\langle\langle A|B\rangle\rangle^r = \langle\{A,B\}\rangle + \langle\langle[A,H]|B\rangle\rangle^r,$$

where A, B are arbitrary operators. Note that the energy ω includes an infinitesimal imaginary part $\mathrm{i}0^{+}$. Applying the equation of motion to the Green function $\langle\langle d_{m\sigma}|d^{\dagger}_{n\sigma'}\rangle\rangle^{r}$, we have

$$\begin{aligned}\omega\langle\langle d_{m\sigma}|d^{\dagger}_{n\sigma'}\rangle\rangle^{r} &= \delta_{mn}\delta_{\sigma\sigma'} + \varepsilon_{m\sigma}\langle\langle d_{m\sigma}|d^{\dagger}_{n\sigma'}\rangle\rangle^{r} \\ &+ U\langle\langle n_{m\bar{\sigma}}(t)d_{m\sigma}(t)|d^{\dagger}_{n\sigma'}\rangle\rangle^{r} \\ &+ (t+\sigma\Delta t)\,\delta_{1m}\langle\langle d_{2\sigma}|d^{\dagger}_{n\sigma'}\rangle\rangle^{r} \\ &+ (t+\sigma\Delta t)\,\delta_{2m}\langle\langle d_{1\sigma}|d^{\dagger}_{n\sigma'}\rangle\rangle^{r} \\ &+ \delta_{1m}\sum_{k} V^{*}_{l1k}\langle\langle c_{lk\sigma}(t)|d^{\dagger}_{n\sigma'}\rangle\rangle^{r} \\ &+ \delta_{2m}\sum_{k} V^{*}_{r2k}\langle\langle c_{rk\sigma}(t)|d^{\dagger}_{n\sigma'}\rangle\rangle^{r}, \end{aligned} \tag{21}$$

where $\bar{m}=2$ when $m=1$, $\bar{\sigma}=\downarrow$ when $\sigma=\uparrow$ and vice versa. Here $\langle\langle n_{m\bar{\sigma}}(t)d_{m\sigma}|d^{\dagger}_{n\sigma'}\rangle\rangle^{r}$ and $\langle\langle c_{\alpha k\sigma}|d^{\dagger}_{n\sigma'}\rangle\rangle^{r}$ are the new Green functions. As usual for an interacting problem, one has also to calculate these new Green functions

$$\begin{aligned}\omega\langle\langle c_{\alpha k\sigma}|d^{\dagger}_{n\sigma'}\rangle\rangle^{r} &= \varepsilon_{\alpha k\sigma}\langle\langle c_{\alpha k\sigma}|d^{\dagger}_{n\sigma'}\rangle\rangle^{r} \\ &+ \delta_{\alpha l}V_{\alpha 1k}\langle\langle d_{1\sigma}|d^{\dagger}_{n\sigma'}\rangle\rangle^{r} + \delta_{\alpha r}V_{\alpha 2k}\langle\langle d_{2\sigma}|d^{\dagger}_{n\sigma'}\rangle\rangle^{r} \end{aligned} \tag{22}$$

$$\begin{aligned}\omega\langle\langle n_{m\bar{\sigma}}d_{m\sigma}|d^{\dagger}_{n\sigma'}\rangle\rangle^{r} &= \delta_{mn}\delta_{\sigma\sigma'}\langle n_{m\bar{\sigma}}\rangle \\ &+ \varepsilon_{m\sigma}\langle\langle n_{m\bar{\sigma}}d_{m\sigma}|d^{\dagger}_{n\sigma'}\rangle\rangle^{r} + U\langle\langle n_{m\bar{\sigma}}d_{m\sigma}(t)|d^{\dagger}_{n\sigma'}\rangle\rangle^{r} \\ &+ \delta_{1m}(t+\sigma\Delta t)\langle\langle n_{1\bar{\sigma}}d_{2\sigma}|d^{\dagger}_{n\sigma'}\rangle\rangle^{r} \\ &+ \delta_{2m}(t+\sigma\Delta t)\langle\langle n_{2\bar{\sigma}}d_{1\sigma}|d^{\dagger}_{n\sigma'}\rangle\rangle^{r} \\ &+ \delta_{1m}\sum_{k} V^{*}_{l1k}\langle\langle n_{1\bar{\sigma}}c_{lk\sigma}|d^{\dagger}_{n\sigma'}\rangle\rangle^{r} \\ &+ \delta_{2m}\sum_{k} V^{*}_{r2k}\langle\langle n_{2\bar{\sigma}}c_{rk\sigma}|d^{\dagger}_{n\sigma'}\rangle\rangle^{r} \\ &- \delta_{1m}\sum_{k} V_{l1k}\langle\langle c^{\dagger}_{lk\bar{\sigma}}d_{m\bar{\sigma}}d_{m\sigma}|d^{\dagger}_{n\sigma'}\rangle\rangle^{r} \\ &- \delta_{1m}\sum_{k} V^{*}_{l1k}\langle\langle c_{lk\bar{\sigma}}d^{\dagger}_{m\bar{\sigma}}d_{m\sigma}|d^{\dagger}_{n\sigma'}\rangle\rangle^{r} \\ &- \delta_{2m}\sum_{k} V_{r2k}\langle\langle c^{\dagger}_{rk\bar{\sigma}}d_{m\bar{\sigma}}d_{m\sigma}|d^{\dagger}_{n\sigma'}\rangle\rangle^{r} \\ &- \delta_{2m}\sum_{k} V^{*}_{r2k}\langle\langle c_{rk\bar{\sigma}}d^{\dagger}_{m\bar{\sigma}}d_{m\sigma}|d^{\dagger}_{n\sigma'}\rangle\rangle^{r} \\ &- \delta_{1m}(t+\bar{\sigma}\Delta t)\langle\langle d^{\dagger}_{2\bar{\sigma}}d_{m\bar{\sigma}}d_{m\sigma}|d^{\dagger}_{n\sigma'}\rangle\rangle^{r} \\ &+ \delta_{1m}(t+\bar{\sigma}\Delta t)\langle\langle d^{\dagger}_{m\bar{\sigma}}d_{2\bar{\sigma}}d_{m\sigma}|d^{\dagger}_{n\sigma'}\rangle\rangle^{r} \\ &- \delta_{2m}(t+\bar{\sigma}\Delta t)\langle\langle d^{\dagger}_{1\bar{\sigma}}d_{m\bar{\sigma}}d_{m\sigma}|d^{\dagger}_{n\sigma'}\rangle\rangle^{r} \\ &+ \delta_{2m}(t+\bar{\sigma}\Delta t)\langle\langle d^{\dagger}_{m\bar{\sigma}}d_{1\bar{\sigma}}d_{m\sigma}|d^{\dagger}_{n\sigma'}\rangle\rangle^{r}. \end{aligned} \tag{23}$$

Now, the Hartree–Fock decoupling scheme is applied to the new Green functions generated on the right-hand side of equation (23),

$$\begin{aligned}\langle\langle n_{m\bar{\sigma}}d_{\bar{m}\sigma}|d^{\dagger}_{n\sigma'}\rangle\rangle^{r} &= \langle n_{m\bar{\sigma}}\rangle\langle\langle d_{\bar{m}\sigma}|d^{\dagger}_{n\sigma'}\rangle\rangle^{r}, \\ \langle\langle n_{m\bar{\sigma}}c_{\alpha k\sigma}|d^{\dagger}_{n\sigma'}\rangle\rangle^{r} &= \langle n_{m\bar{\sigma}}\rangle\langle\langle c_{\alpha k\sigma}|d^{\dagger}_{n\sigma'}\rangle\rangle^{r}, \end{aligned} \tag{24}$$

and set

$$\begin{aligned}\langle\langle d^{\dagger}_{\bar{m}\bar{\sigma}}d_{m\bar{\sigma}}d_{m\sigma}|d^{\dagger}_{n\sigma'}\rangle\rangle^{r} &= 0, \\ \langle\langle d^{\dagger}_{m\bar{\sigma}}d_{\bar{m}\bar{\sigma}}d_{m\sigma}|d^{\dagger}_{n\sigma'}\rangle\rangle^{r} &= 0, \\ \langle\langle c_{\alpha k\bar{\sigma}}d^{\dagger}_{m\bar{\sigma}}d_{m\sigma}|d^{\dagger}_{n\sigma'}\rangle\rangle^{r} &= 0, \\ \langle\langle c^{\dagger}_{\alpha k\bar{\sigma}}d_{m\bar{\sigma}}d_{m\sigma}|d^{\dagger}_{n\sigma'}\rangle\rangle^{r} &= 0, \end{aligned} \tag{25}$$

which closes the set of equations (21)–(23) and the compact form can be written as the Dyson equation (equation (6)) with the self-energy equation (12).

References

[1] Prinz G 1998 *Science* **282** 1660
Wolf S A *et al* 2001 *Science* **294** 1488
[2] Zutic I, Fabian J and Das Sarma S 2004 *Rev. Mod. Phys.* **76** 323
[3] Hammar P R, Bennett B R, Yang M J and Johnson M 1999 *Phys. Rev. Lett.* **83** 203
[4] Fiederling R *et al* 1999 *Nature* **402** 787
[5] Ohno Y *et al* 1999 *Nature* **402** 790
[6] Jiang X *et al* 2003 *Phys. Rev. Lett.* **90** 256603
[7] Hirsch J E 1999 *Phys. Rev. Lett.* **83** 1834
[8] Pareek T P 2004 *Phys. Rev. Lett.* **92** 076601
[9] Murakami S *et al* 2003 *Science* **301** 1348
[10] Sinova J *et al* 2004 *Phys. Rev. Lett.* **92** 126603
[11] Mireles F and Kirczenow G 2001 *Phys. Rev.* B **64** 024426
[12] Sergueev N, Sun Q F, Guo H, Wang B G and Wang J 2002 *Phys. Rev.* B **65** 165303
[13] Wang B, Wang J and Guo H 2003 *Phys. Rev.* B **67** 092408
[14] Zhang P, Xue Q K, Wang Y P and Xie X C 2002 *Phys. Rev. Lett.* **89** 286803
[15] Martinek J *et al* 2003 *Phys. Rev. Lett.* **91** 127203
[16] Fransson J, Holmström E and Eriksson O 2003 *Phys. Rev.* B **67** 205310
[17] Hüttel A K, Ludwig S, Lorenz H, Eberl K and Kotthaus J P 2005 *Phys. Rev.* B **72** 081310
[18] Buttiker M 1983 *Phys. Rev.* B **27** 6178
[19] Jauho A P, Wingreen N S and Meir Y 1994 *Phys. Rev.* B **50** 5528
[20] van der Vaart N C *et al* 1995 *Phys. Rev. Lett.* **74** 4702
[21] Langreth D C 1976 *Linear and Nonlinear Electron Transport in Solid* ed J T Devreese and E van Doren (New York: Plenum)